CERN – EUROPEAN ORGANIZATION FOR NUCLEAR RESEARCH

CLIC – Note – 1157

LOCALIZATION OF VACUUM BREAKDOWN LOCATIONS IN RF STRUCTURES USING S-PARAMETER DATA

C. H. Wu[1,2] and J. Paszkiewicz[1,2]

[1]University of Oxford, Oxford, UK, OX1 3PU
[2]CERN, Geneva, Switzerland

CERN-ACC-2020-0006
04/11/2019

Abstract

This project is an investigation to find the breakdown locations using a new method involving group delays of the Scattering parameters (or S-parameters). The RF signals of the T24PSI 1 from the Xbox-2 test stand at CERN have been used to parasitically estimate the S-parameters of the structure during high-power testing. The derivative of these parameters with respect to frequency are calculated to find the group delays, which lead to the breakdown locations. It is found that the method has worked perfectly well on normal pulses, and has reproduced the length of the test structure as the distance travelled. When the method is applied on breakdown pulses, the noise and the complex nature of breakdowns, with unknown reasons, have undermined the capability of the method in calculating the correct breakdown locations.

Geneva, Switzerland
4 November 2019

1 CLIC and Xbox2

The Compact Linear Collider (CLIC) study is an international collaboration to develop the future electron-positron collider with energies up to several TeV and its aim is to explore the frontiers of high-energy physics. Radiofrequency (RF) structures are used to provide high-gradient electric fields such that electrons and positrons, with masses of 0.511MeV/c^2, could be accelerated up to a centre of mass energy of 3 TeV [1]. The CLIC project provides an alternative approach to the Large Hadron Collide (LHC) to find new physics as it collides leptons instead of hadrons, and comes with better precision.

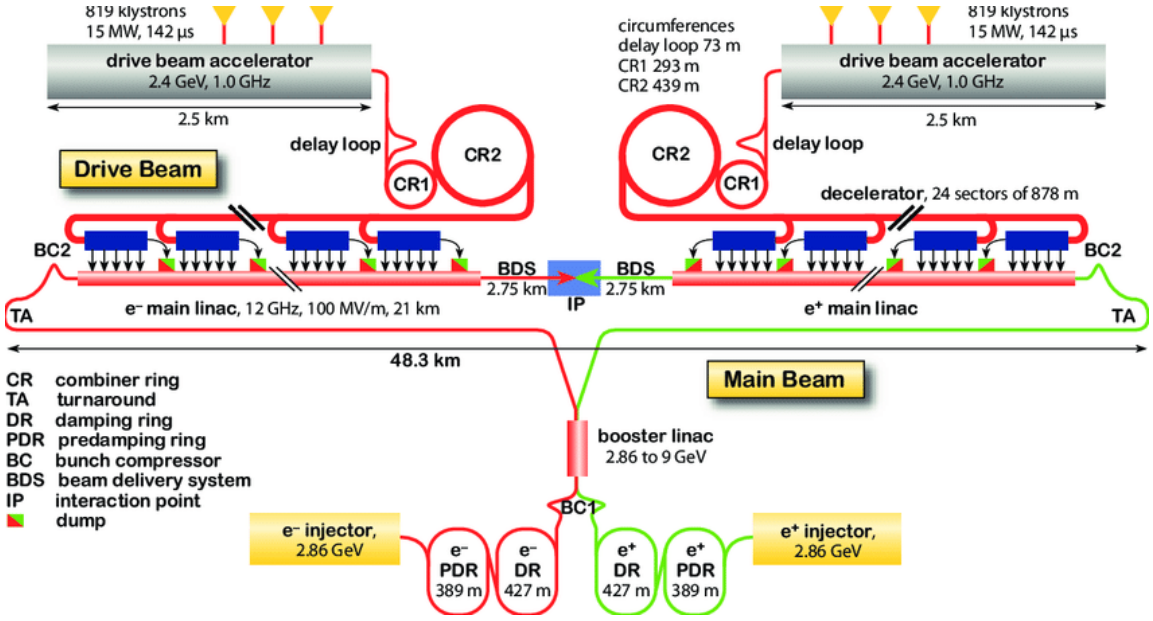

Figure 1: CLIC layout diagram at 3 TeV

To operate at high gradient, the structure has to overcome the challenges of vacuum breakdowns. The maximum breakdown rate (BDR) specification for CLIC at 3 TeV is about 3×10^{-7} bpp/m [2]. Three "Xbox" test stands are set up at CERN to test the high accelerating gradient with prototype structures for long periods of time to aid with R&D [3]. The data obtained from Xbox-2 has been analysed using Matlab and the results are presented in the following sections.

In Xbox-2, the low-level RF (LLRF) system demodulates signals from directional couplers, which allow high power RF pulses to be measured [4]. The klystron produces up to 50 MW power pulses at 11.994 GHz of $1.5\mu s$ length at a repetition rate of 50 Hz.

The amplitudes and phases of the incident, reflected and transmitted pulses are saved to memory every minute when no breakdown occurs. If a breakdown occurs, the device records the data of the breakdown pulse together with the two previous pulses (i.e. 20 ms and 40 ms respectively before the breakdown pulse) [2, 3].

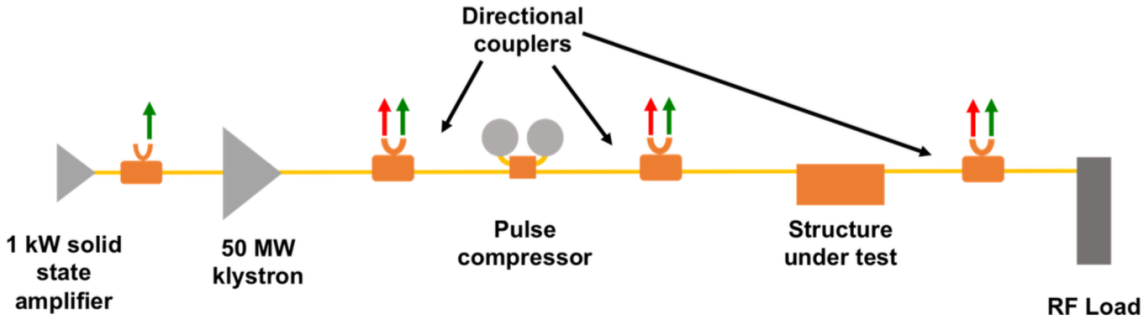

Figure 2: Block diagram of the Xbox 2 test stand. Adapted from [5]

2 Conditioning and breakdowns

A conditioning process is carried out before the structure is ready for high gradient such as 100 MV/m in order to clean field emission sites and impurities on the copper surface as they play a role in the breakdown process [6, 7]. The process is controlled by an algorithm such that the gradient starts from 0 MV/m, and slowly increases once the BDR at each gradient falls below a certain level, indicating that the structure is ready to be exposed to the next higher gradient.

Breakdowns are very complicated physical phenomenon that occurs due to the high field gradient within the RF cavity. It involves many fields of applied physics such as surface, material and plasma physics etc... The exact mechanism is in fact not known yet [8].

The relationship between breakdown rate (BDR) and accelerating field has been found follow a power law of BDR $\propto E_{\text{acc}}^{30}$ [8]. When breakdown occurs, it acts like a conductive plasma wall which forms a short circuit [9], then blocks and reflects all incident waves, and this could be seen in figure 3a where the amplitude of the transmitted signal exiting the structure, the |PEI| signal, rapidly falls to zero.

A common method to find the breakdown locations is called the "Edge Method", it uses the propagation delay of signals through the structure, on the order of around 1% of speed of light [10]. In this project, an alternative approach which utilises the RF

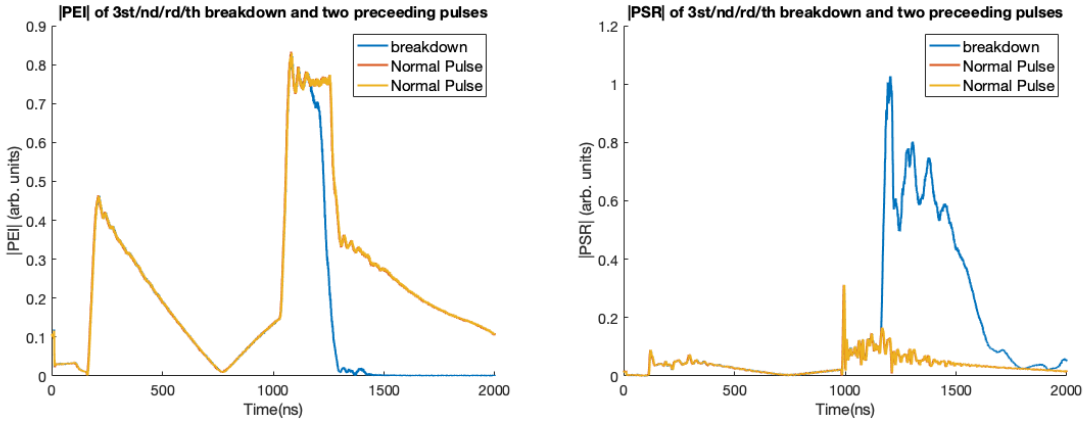

(a) Structure Transmitted Amplitude |PEI| pulse (b) Structure Reflected Amplitude |PSR| pulse

Figure 3: Comparison between breakdown pulses and two preceding normal pulses. Note that the two normal pulses are almost identical therefore one overlaps the other.

signals recored at the Xbox2 is used to calculate the breakdown locations. The findings are explained in the following sections.

3 Normal pulses

Based on previous work done by Kathryn Jones [11], the Matlab script to analyse normal pulses has been adapted and improved. The calculations of the S-parameters S_{11} and S_{21} of the structure under test have shown to match the 3D electromagnetic simulations performed in the High Frequency Structure Simulator (HFSS) (figure 6).
The estimates of S_{11} and S_{21} are given by

$$\widehat{S_{11}}(\omega) = \frac{\mathrm{FT}\big[h(t)\cdot \mathrm{PSR}(t)\big]}{\mathrm{FT}\big[h(t)\cdot \mathrm{PSI}(t)\big]} \qquad \text{and} \qquad \widehat{S_{21}}(\omega) = \frac{\mathrm{FT}\big[h(t)\cdot \mathrm{PEI}(t)\big]}{\mathrm{FT}\big[h(t)\cdot \mathrm{PSI}(t)\big]} \tag{1}$$

,where FT refers to the Fourier transforms on the signal, PSI refers to the Structure Input. A Hann window $h(t)$ has been applied to each signal before taking the Fourier Transform because the waveforms are not periodic in time, and this would add high-order frequency terms to the result [12].

3.1 Waveforms of a single pulse

As shown in figure 4a, a typical pulse lasts about $1.1\mu s$ but the main peak of 50 MW starts 900ns from the start of the pulse and lasts for 200 ns. The structure has a passband of 0.1 GHz and minimum reflection is at the operation frequency of 11.994 GHz (figure 5a).

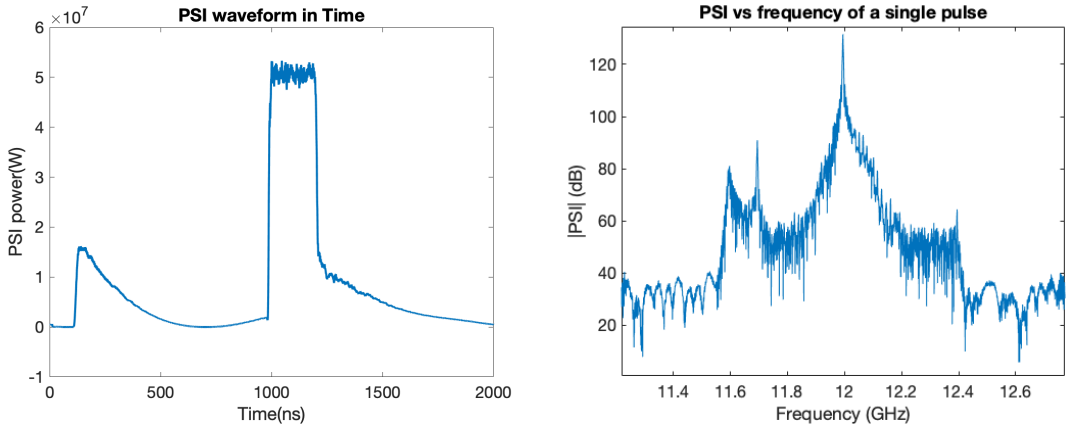

(a) PSI vs time

(b) PSI vs frequency

Figure 4: |PSI| of a single pulse in both time and frequency domains.

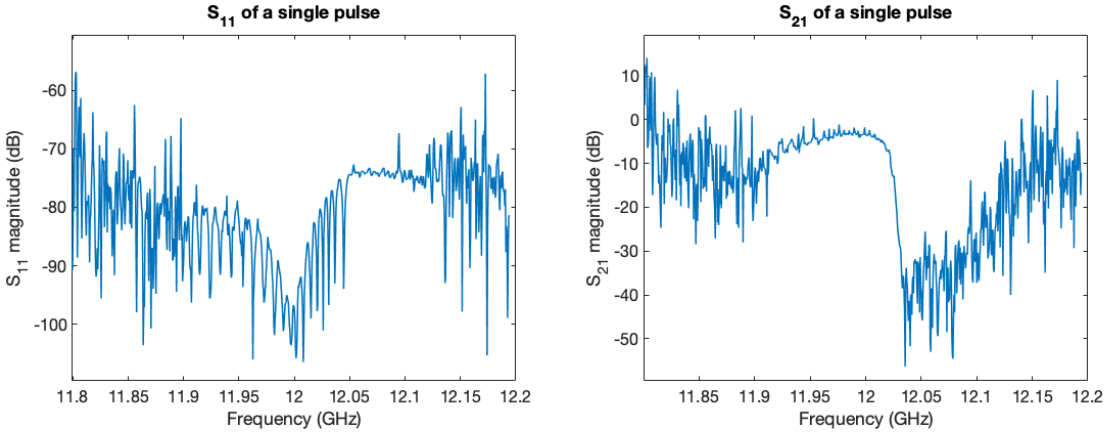

(a) S_{11} parameter.

(b) S_{21} parameter

Figure 5: S-parameters of a single pulse. As the reflected signal S_{11} is scaled by unknown constant, a shift occurs on the vertical axis of (a)

3.2 Averaging normal pulses

From figure 5, significant level of noise has been observed at frequencies more than ±0.05 GHz away from the central frequency 11.994 GHz. The reason for this is the low signal to noise (V to N in (2)) ratio (see figure 4b), which means that the S-parameters would have poor accuracies in these frequencies. It would be beneficial to calculate an average of pulses to obtain a smoother graph for analysis as it helps cancelling the randomly noise. The expression of the averaged S-parameters of M pulses is given by

$$\bar{S}_{ij}(\omega) = \frac{1}{M}\sum_{k=1}^{M} S_{ij}^{k}(\omega) = \frac{1}{M}\sum_{k=1}^{M}\left(\frac{V_i^+(\omega)+N_i(\omega)}{V_j^-(\omega)+N_j(\omega)}\right)_k \tag{2}$$

, where V^+ and V^- refer to input to and output respectively, and N refers to the noise. Both averaged S_{11} and S_{21} values have been plotted in figure 6, together with the values of a single pulse and the simulated data from HFSS. It is seen that the averaging of pulses allows us to fit the direct measurement down to 11.88 GHz.

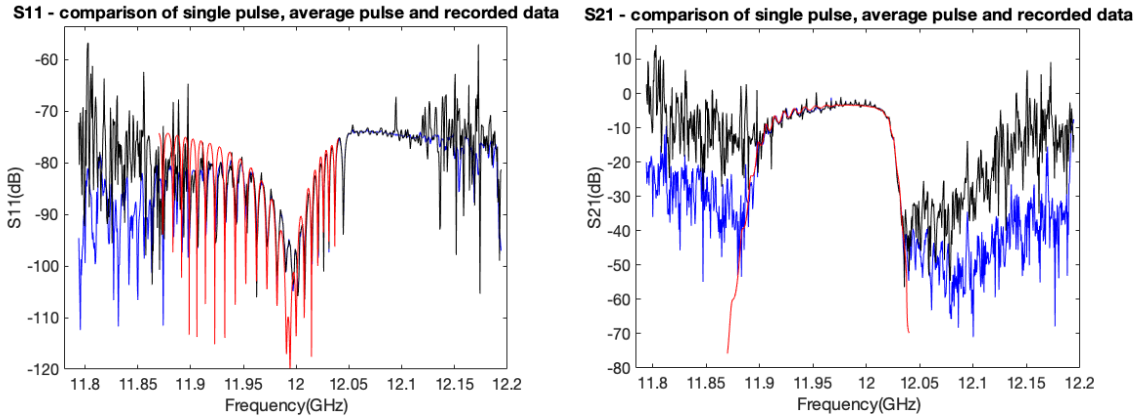

(a) S_{11} parameter

(b) S_{21} parameter

Figure 6: S-parameters derived from a single pulse (black), an averaged of multiple pulses (blue) and simulation (red)

3.3 Applying the group delay method to averaged normal pulse

By taking derivatives of the phases $arg(S_{21})$ with respect to frequency, it is possible to find the group delay with the following expression:

$$\text{Group Delay } \tau_g \text{ (ns)} \ = -\frac{\partial arg(S_{21})}{\partial \omega} \tag{3}$$

[13]. Theoretically, the equation would produce the time taken for the pulses to travel through the structure when there are no breakdowns.

3.3.1 Unwrapping arg(S_{ij}) and find slope

From figure 7 it could be seen that arg(S_{11}) is rather noisy. Taking the derivative of arg(S_{ij}) produces a spike every time the phase jumps between π and $-\pi$. Unwrapping arg(S_{ij}) removes discontinuities so that derivative is taken on a much smoother curve. The expression of this method is given by

$$\tau_g = \frac{1}{\Delta\omega}(\arg(S_{21}(\omega + \Delta\omega)) - \arg(S_{21}(\omega))), \tag{4}$$

where $\Delta\omega$ is the frequency resolution. The method is first applied onto the normal pulses to check if it gives us the expect value of around $65ns$, which is the expected design value of group delay of the structure. By taking the slope of the arg(S_{21}) within the region of 11.95 GHz to 12.01 GHz (see figure 8a), a distribution of group delays around 65.4ns $\pm$ 0.1ns was found and this is shown in figure 8b. This is consistent with the structure's design parameters and it shows a convincing potential towards the search of breakdown locations.

3.3.2 Alternative approach

Another method to find the derivative is to find the angle of the division between two adjacent $S_{11}(\omega)$ values. The expression is given by:

$$\tau_g = \frac{1}{\Delta\omega}\arg\left(\frac{S_{21}(\omega + \Delta\omega)}{S_{21}(\omega)}\right). \tag{5}$$

It is found that this has equivalent performance to the first method with unwrapping, this is because that both considered the angular difference between two adjacent $S_{11}(\omega)$ values. Yet it is possible that this gives different values when the unwrap function misidentify jumps due to fluctuations.

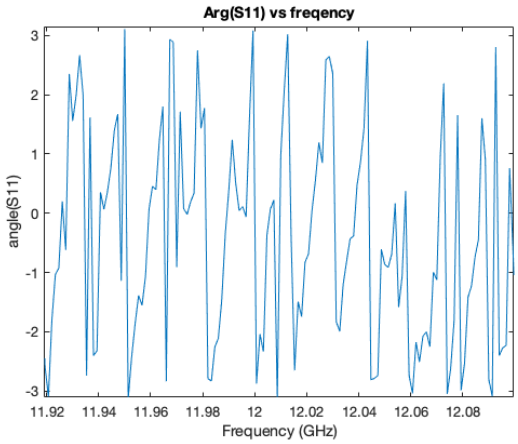

Figure 7: Wrapped $arg(S_{11})$ plot. It is hard to find the slope of this plot.

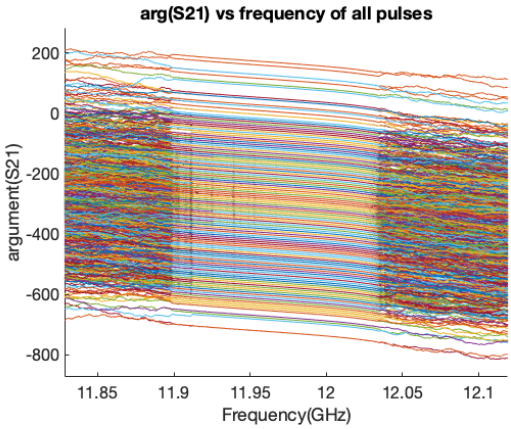

(a) arg(S_{21}) unwrapped

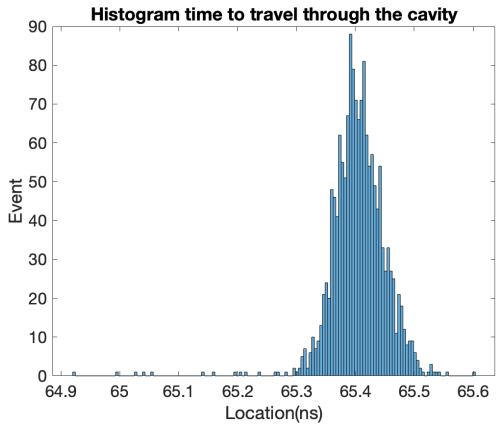

(b) Breakdown Locations

Figure 8: Results of the method on normal pulses

4 Analysis of Breakdown pulses

The same methods have been applied to breakdown pulses with the aim to find the breakdown location. When breakdown occurs, conductive plasma that reflects all the pulses is formed [9], hence to find the breakdown location one has to consider S_{11} instead. The main amendments made is to trim the PSR, PSI and PEI pulses, so that only the time window after the breakdown occurred is fourier tranformed. This is due to the Linear Time Invariant assumption which is necessary for the s-parameter formalism to work. A further factor of $\frac{1}{2}$ accounts for the fact that the pulses travelled twice the distance to return to origin. The expression is now given by:

$$\text{Breakdown position from input (time unit)} = -\frac{1}{2}\frac{\partial arg(S_{11})}{\partial \omega}. \tag{6}$$

4.1 Results using previous methods

With this method, data from October 2017 to March 2018 of the testing of T24PSI 1 structure in Xbox-2 has been used to calculate the group delay. A histogram summarising the results has been plotted in figure 9a. The shape of distribution of the breakdown locations is in fact very similar to that in [14]. The width of distribution is around 70ns, matching the length of the structure. However the plot spans from -40 ns to 30 ns, and negative propagation delay is unphysical.

Following the findings, extra effort has been put in to compare the results from the

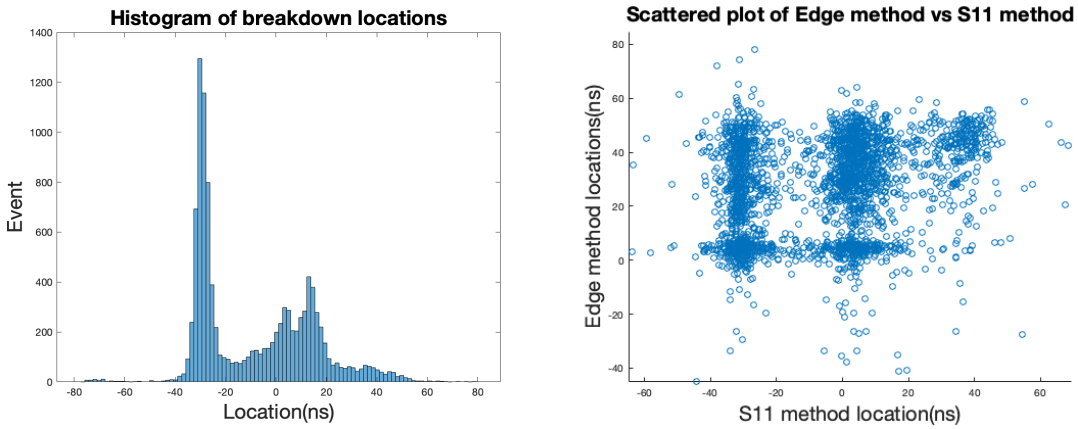

(a) Histogram of breakdown locations of all data (b) Scattered plot using November 1-20 data

Figure 9: Results of the method on breakdown pulses

edge method and the group delay method. The scatter plot in figure 9b shows that there is in fact no correlation between locations found by two methods, meaning that the results above, with similar distribution to that of the edge method, is likely to be a coincidence.

4.2 Further attempts and result

4.2.1 Removing spikes and smoothing

From figure 9b, we can see that the breakdown locations are in fact grouped into multiple clusters, and this is because of the strong spikes created when taking the derivative of $arg(\mathrm{S}_{11})$ (see figure 10). An attempt to solve this problem is to take the derivative of a wrapped angle of S_{11} then remove the spikes and fit histogram on the remaining data. Another improvement is to smooth the curve before taking derivative has been carried out. From figure 10, it is shown that after unwarpping and smoothing (green line), the slope is now much more steady.

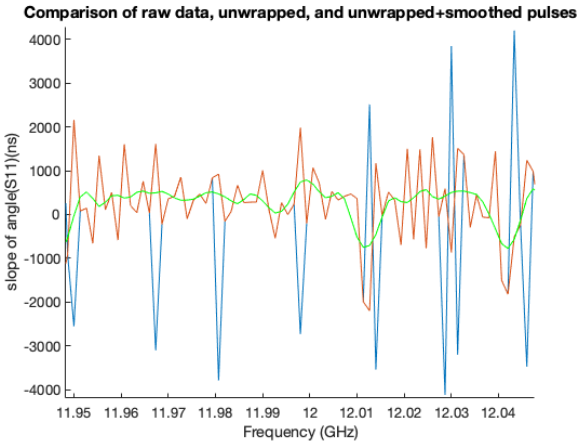

Figure 10: Raw data (Blue), Unwrapped (Orange), Unwrapped and smoothed (Green)

4.2.2 diff(wrapped arg($S_{11}(\omega)$)), remove spikes and calculate mean

The fluctuations that caused jumps in the plot of S_{11} (see figure 10) has led to spikes in finding the slope of the curve. Since the mean of the slopes within a specific range of frequencies is taken, it explains why the results are grouped into clusters. One way to solve the problem is to remove the spikes that greatly skewed the mean. With this method applied, only a broad distribution around -40ns is found (see figure 11a). This confirms that the disappearance of the other two peaks is due to the removal of strong spikes that decreases the mean. However, there remains no correlation between the locations calculated by two distinct methods (see figure 11b).

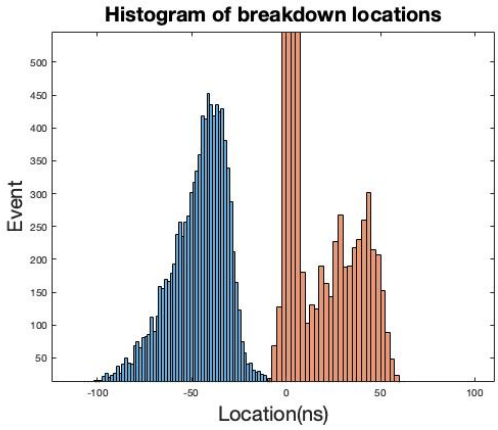

(a) Edge vs group method location. Orange refers to edge method, whose peak around 0 ns reaches 3000 (beyond the figure).

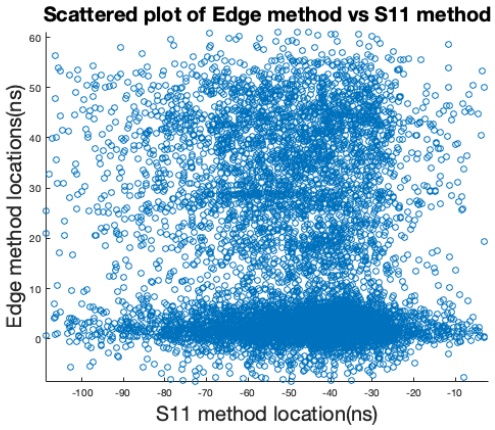

(b) Scatted plot showing no correlation between results from two methods after spikes removal of all data.

Figure 11

4.3 Conclusion

It is clear that the breakdown process is very complicated and rather unpredictable. It appears that, in the analysis of breakdown pulses, arguments of $S_{11}(\omega)$ of most pulses share the same positive slope around 12 GHz (see figure 12a) which implies a negative breakdown location around -35 ns. This contradicts the results from edge method location as there should be some slopes at least 40 times steeper than the others (for breakdowns around 40 ns and 1 ns respectively), and all slopes should be negative. Further investigation should be carried out on this matter. In fact, Dr. Robin Rajamäki have shown convincing results by applying a correlation method on the same information [15], which hold promise to the success of the group delay method. Therefore, I believe with more rigorous treatment, our method would be capable of determining the breakdown locations at appropriate accuracies.

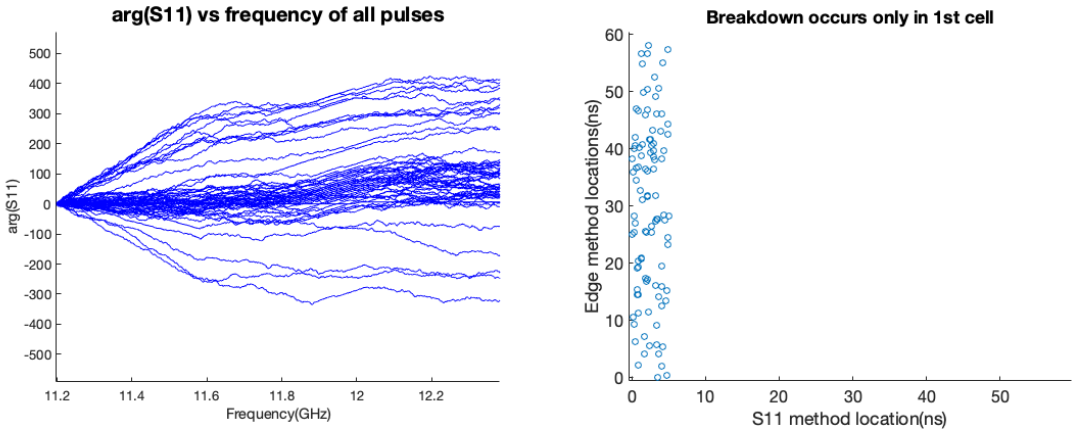

(a) Unwrapped arg(S_{11}) of BDs on 2018-03-02 (b) Scatter plot if breakdown stays in 1st cell

Figure 12

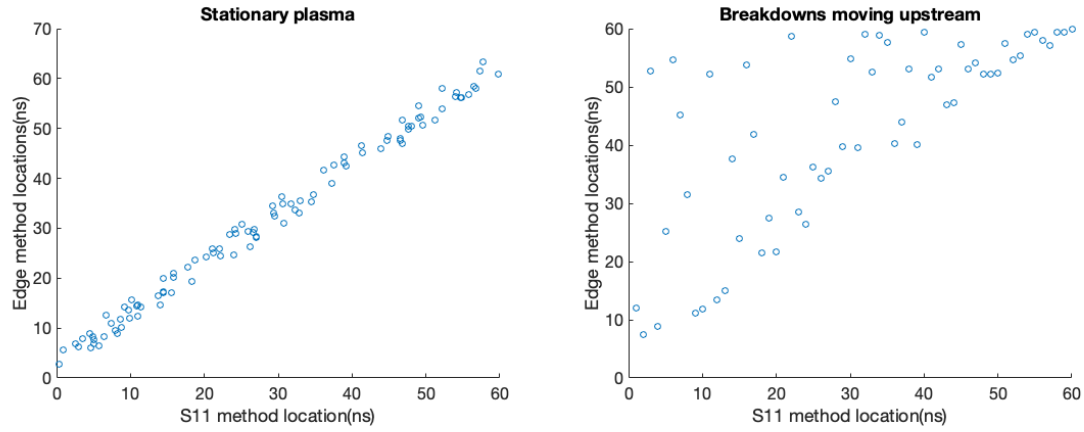

(a) Ideal scatter plot with stationary breakdown (b) If breakdown moves upstream

Figure 13: Scatter plot of hypothetical situations

5 Potential research direction

5.1 Moving plasma

In some part of this study, it was found that the stable slope around 12GHz has been shifted by 0.05GHz. This raises the question of whether the conductive plasma was moving or expanding, leading to the doppler shift of the reflected pulse.

5.2 Inverse Fourier transform of $S_{11}(\omega)$ and $S_{21}(\omega)$

In the above method, $S_{11}(\omega)$ and $S_{21}(\omega)$ have been calculated using the fourier transformed data of PEI,PSI and PSR. By the end of the project there was the idea to perform an inverse Fourier Transform of $S_{11}(\omega)$ and $S_{21}(\omega)$ in order to find the breakdown locations. With this method applied, a strong peak of transmitted pulse $S_{21}(t)$ around 60 ns was observed (see figure 11). In addition to that, other peaks are detected, this is possibly due to the multiple reflections between various impedance boundaries such as the structure input and output, pulse compressor and klystron output. These boundaries lead to many possible paths and hence multiple peaks on the impulse response plot.

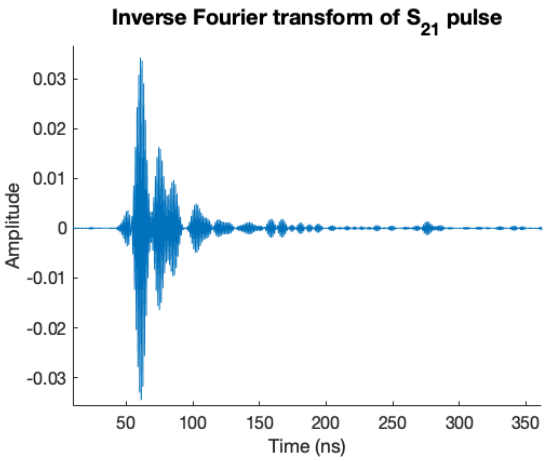

Figure 14: Inverse fast fourier transform of S_{21} of normal pulse

6 Acknowledgement

I gratefully thank Jan for his continuous support and comments throughout the past few months and Prof. Burrows for the opportunity to work on this project at CERN. I would also like to thank Martin, Judita, Clara, Santi, Khaled, Daniel and many others who gave me ideas during the summer programme at CERN.

References

[1] M Aicheler, P Burrows, M Draper, T Garvey, P Lebrun, K Peach, N Phinney, H Schmickler, D Schulte, and N Toge. *A Multi-TeV Linear Collider Based on CLIC Technology: CLIC Conceptual Design Report*. CERN Yellow Reports: Monographs. CERN, Geneva, 2012.

[2] Eugenio Senes, Theodoros Argyropoulos, Frank Tecker, and Walter Wuensch. Beam-loading effect on breakdown rate in high-gradient accelerating cavities: An experiment at the Compact Linear Collider Test Facility at CERN. *Phys. Rev. Accel. Beams*, 21(10):102001. 8 p, 2018.

[3] Phil Burrows, Walter Wuensch, and Theodoros Argyropoulos. High-gradient x-band rf technology for clic and beyond. *Proceedings of 38th International Conference on High Energy Physics — PoS(ICHEP2016)*, Apr 2017.

[4] Benjamin Woolley, Praveen Kumar Ambattu, Robert Apsimon, Graeme Burt, Amos Dexter, Alexej Grudiev, Igor Syratchev, Rolf Wegner, and Walter Wuensch. High Gradient Testing of an X-band Crab Cavity at XBox2. *Proceedings of IPAC2015, Richmond, VA, USA*, 2015.

[5] J. Paszkiewicz. X-band rf test stands at cern. PowerPoint presentation.

[6] Benjamin J. Woolley. *High Power X-band RF Test Stand Development and High Power Testing of the CLIC Crab Cavity*. PhD thesis, Lancaster U., 2015.

[7] Walter Wuensch. A review of vacuum breakdown in high-gradient accelerators. In *2018 28th International Symposium on Discharges and Electrical Insulation in Vacuum (ISDEIV)*, pages 747–752, 09 2018.

[8] A Grudiev and W Wuensch. A new local field quantity describing the high gradient limit of accelerating structures. Technical Report CERN-OPEN-2009-015. CLIC-Note-772, CERN, Geneva, Oct 2008.

[9] Helga Timko. *Modelling vacuum arcs: from plasma initiation to surface interactions*. PhD thesis, Helsinki U., 2011.

[10] Alberto Degiovanni, Steffen Döbert, Wilfrid Farabolini, Igor Syratchev, Walter Wuensch, Jorge Giner Navarro, Joseph Tagg, and Benjamin Woolley. Diagnostics and Analysis Techniques for High Power X-Band Accelerating Structures. *Proceedings of LINAC2014, Geneve, Switzerland*, 2014.

[11] Kathryn Jones. Investigating a new method to find s-parameters and breakdown positions in radio frequency cavities. CERN Summer Student Project Report, 2018.

[12] M Gasior, M Guinchard, A Kuzmin, J Pfingstner, H Schmickler, M Sylte, M Billing, M Böge, and M Dehler. Sub-NM Beam Motion Analysis using a Standard BPM with High Resolution Electronics. Technical Report CERN-BE-2010-012, CERN, Geneva, May 2010.

[13] J. Blauert and P. Laws. Group delay distortions in electroacoustical systems. *The Journal of the Acoustical Society of America*, 63(5):1478–1483, May 1978.

[14] Jan Paszkiewicz, Philip Burrows, and Walter Wuensch. Spatially resolved dark current in high gradient traveling wave structures. page WEPRB062. 4 p, 2019.

[15] Robin Rajamaki. Vacuum arc localization in CLIC prototype radio frequency accelerating structures. Master's thesis, Aalto U., 2016-03-14.